Long non-coding RNA colon cancer-associated transcript 1-Vimentin axis promoting the migration and invasion of HeLa cells

Zhangfu Li[1], Jiangbei Yuan[1], Qingen Da[1,2], Zilong Yan[1], Jianhua Qu[3], Dan Li[4], Xu Liu[3], Qimin Zhan[4,5], Jikui Liu[3]

[1]Department of Hepato-Pancreato-Biliary Surgery, Peking University Shenzhen Hospital, Shenzhen Peking University-The Hong Kong University of Science and Technology Medical Center, Shenzhen, Guangdong 518036, China;
[2]Department of Cardiovascular Surgery, Peking University Shenzhen Hospital, Shenzhen Peking University-The Hong Kong University of Science and Technology Medical Center, Shenzhen, Guangdong 518036, China;
[3]Department of Hepato-Pancreato-Biliary Surgery, Peking University Shenzhen Hospital, Shenzhen, Guangdong 518036, China;
[4]State Key Laboratory of Molecular Oncology, National Cancer Institute and Cancer Hospital, Chinese Academy of Medical Sciences and Peking Union Medical College, Beijing 100021, China;
[5]Key Laboratory of Carcinogenesis and Translational Research (Ministry of Education/Beijing), Laboratory of Molecular Oncology, Peking University Cancer Hospital & Institute, Beijing 100142, China.

Abstract

Background: Long non-coding RNA colon cancer-associated transcript 1 (CCAT1) is involved in transforming multiple cancers into malignant cancer types. Previous studies underlining the mechanisms of the functions of CCAT1 primarily focused on its decoy for miRNAs (micro RNAs). However, the regulatory mechanism of CCAT1–protein interaction associated with tumor metastasis is still largely unknown. The present study aimed to identify proteome-wide CCAT1 partners and explored the CCAT1–protein interaction mediated tumor metastasis.

Methods: CCAT1–proteins complexes were purified and identified using RNA antisense purification coupled with the mass spectrometry (RAP-MS) method. The database for annotation, visualization, and integrated discovery and database for eukaryotic RNA binding proteins (EuRBPDB) websites were used to bioinformatic analyzing CCAT1 binding proteins. RNA pull-down and RNA immunoprecipitation were used to validate CCAT1–Vimentin interaction. Transwell assay was used to evaluate the migration and invasion abilities of HeLa cells.

Results: RAP-MS method worked well by culturing cells with nucleoside analog 4-thiouridine, and cross-linking was performed using 365 nm wavelength ultraviolet. There were 631 proteins identified, out of which about 60% were RNA binding proteins recorded by the EuRBPDB database. Vimentin was one of the CCAT1 binding proteins and participated in the tumor metastasis pathway. Knocked down vimetin (*VIM*) and rescued the downregulation by overexpressing CCAT1 demonstrated that CCAT1 could enhance tumor migration and invasion abilities by stabilizing Vimentin protein.

Conclusion: CCAT1 may bind with and stabilize Vimentin protein, thus enhancing cancer cell migration and invasion abilities.

Keywords: lncRNA CCAT1; RAP-MS; RNA binding protein; Vimentin; Migration; Invasion

Introduction

Colon cancer-associated transcript 1 (CCAT1) is an oncogenic long non-coding RNA (lncRNA) located at 8q24.21, a commonly amplified genomic area in various human cancers.[1] Consistent with this, multiple human cancer tissues show a higher CCAT1 expression than the corresponding adjacent normal tissues.[2] Studies have identified that CCAT1 is highly involved in migration, invasion, proliferation, and chemoresistance in cancer development.[3-5] Mechanistically, CCAT1 may regulate gene expression by binding with transcriptional factors that influence the promoter activity of target genes.[6,7] CCAT1 also serves as a competing endogenous RNA to sponge miRNAs that affect kinase signaling regulatory pathways.[4,8,9] Recently, several studies have focused on lncRNA–protein interactions to regulate cell signaling transduction.[10] Therefore, elucidating the oncogenic role of CCAT1 from the perspective of CCAT1–protein interaction presents a meaningful and necessary scientific question.

Access this article online

Quick Response Code:

Website: www.cmj.org

DOI: 10.1097/CM9.0000000000002373

Correspondence to: Jikui Liu, Department of Hepato-Pancreato-Biliary Surgery, Peking University Shenzhen Hospital, Shenzhen, Guangdong 518036, China
E-Mail: liu8929@126.com

Chinese Medical Journal 2023;136(19)
Received: 24-10-2022; **Online:** 29-03-2023 **Edited by:** Jing Ni

RNA binding proteins (RBPs) are generally considered as proteins that change the fate or function of their bound RNAs. RBPs interact with RNAs typically by one or multiple RNA-binding domains (RBDs), including the RNA recognition motif (RRM), heterogeneous nuclear ribonucleoprotein K homology, and DEAD-box helicase domain.[11] RBPs with well-defined RBDs are referred to as canonical-RBPs. More recently, combinations of *in situ* RNA-protein crosslinking and quantitative mass spectrometry methods have emerged, which help to identify proteome-wide RBPs, yielding large numbers of novel RBPs that defy convention by lacking discernible RBDs.[12] RNA antisense purification coupled with mass spectrometry (RAP–MS) is the most interesting among proteome-wide RBP identification methods.[13,14] RAP-MS uses direct RNA-protein cross-linking coupled with enhanced denaturing purification conditions, providing proteome-wide high-confidence protein interactions.

Vimentin is a primary kind of intermediate filament protein and involves in tumor cells' epithelial-to-mesenchymal transition (EMT) process.[15] It formed an intermediate filament to maintain the mechanical properties and contractility of cells. Vimentin also participates in cell skeleton regulation, lipid metabolism, and pathogen recognition.[16] Interestingly, Vimentin is a vital non-canonical RBP and is bound by several lncRNAs that affect cells' migration ability.[17-19]

Our study aimed to identify proteome-wide CCAT1 binding proteins and to explore the possibilities that CCAT1–protein interactions have an oncogenic role. To achieve this goal, a modified RAP–MS protocol was performed to identify proteome-wide CCAT1 binding proteins. How CCAT1–protein interaction effecting on the migration and invasion abilities of HeLa cells was furtherly discussed in this study.

Methods

Cell culture

HeLa cell was purchased from the Cell Culture Center, Chinese Academy of Medical Sciences (Beijing, China). A stable HeLa-Nlp cell was generated by professor Zhan's laboratory.[20] HeLa and HeLa-derived cells were grown in high glucose Dulbecco's modified eagle medium (DMEM) (Catalog No. 11995065, Gibco, Thermo Fisher Scientific, Waltham, USA) supplemented with 10% fetal bovine serum (Catalog No. 10100-147, Gibco, Thermo Fisher Scientific) at 37°C in humidified air with 5% CO_2.

Chemicals and reagents

Nucleoside analog 4-thiouridine (4sU; Catalog No. T4509, Sigma, St. Louis, USA), lithium chloride solution (Catalog No. L7026-100 ml, Sigma), dodecyl maltoside (Catalog No. D4641-1G, Sigma), sodium dodecyl sulfate (Catalog No. A100227-0100, Sangon Biotech, Shanghai, China), protease inhibitor cocktail (Catalog No. P8340-1ML, Sigma), RNase inhibitor (Catalog No. AM2684, Invitrogen, Thermo Fisher Scientific), streptavidin-coated magnetic beads (Catalog No. 65001, Invitrogen), and benzonase (Catalog No. E8263, Sigma) were the chemicals and reagents used in this study.

RAP–MS

To capture endogenous CCAT1–protein complexes, we designed and synthesized 5′ biotinylated 90-mer antisense DNA oligonucleotides probes (Sangon Biotech). Probes tiled across CCAT1 sequence without overlapping (details were given in Supplementary Table 1, http://links.lww.com/CM9/B243). We grew 40 million HeLa and 20 million HeLa-Nlp cells for CCAT1 antisense purification. The following steps were performed as previously described[21] with slight modification. Cells were cultured to approximately 80% confluence. Nucleoside analog 4sU was added to culture media at a final concentration of 100 μmol/L. Overnight treatment (about 16 h) ensured largely uniform labeling of the cell RNAs. Culture media was then discarded, and cells were washed twice with ice-cold phosphate buffer saline (PBS). HeLa and HeLa-Nlp cells were cross-linked under 0.8 J/cm^2 of ultraviolet (UV) light at a wavelength of 365 nm and harvested for subsequent experiments. As a control, part of HeLa cells was cross-linked under 0.8 J/cm^2 of UV light at a wavelength of 254 nm. Cells were lysed by 900 μL total cell lysis buffer and incubated on ice for 10 min. Then, cell samples were passed through a 26-G needle and sonicated by a sonicator. Then the cell lysates were mixed with twice the volume of 1.5 × hybridization buffer and incubated for 10 min. The samples were centrifuged for 10 min, 12,000×*g* at 4°C. The supernatant lysates could store at −80°C or be used to perform RNA-protein complexes pulling-down. The lysates were first mixed with streptavidin-coated magnetic beads (Catalog No. 65001, Invitrogen) for pre-clearing. About 10,000 cells worth of lysate was retained as the RNA input sample. The following step is hybridization. Probes (2 μg) were denatured and mixed with lysate. Those mixtures were incubated for 2 h at 67°C with intermittently mixing. During this time, 120 μL of streptavidin-coated magnetic beads were prepared for each sample. About 10,000 cells worth of lysate mixture was retained as the RNA input + probe sample. Then the lysate mixtures were mixed with streptavidin-coated magnetic beads washed before. Those complexes were incubated for 30 min at 67°C. Probes–RNA–protein complexes containing beads were magnetically separated, and the supernatants were removed. About 10,000 cells worth of supernatant was retained as the RNA flow-through sample. Beads were washed six times with 1 × hybridization buffer. About 1% of the total volume beads were retained as the RNA elution sample. The rest of the beads was resuspended by 100 μL of Benzonase elution buffer and incubated for 2 h at 37°C. The beads and supernatants were magnetically separated. Eluted proteins in the supernatants were reserved and identified by mass spectrometry. Mass spectrometry was performed by Capital Biotech (Beijing, China). Proteins were identified by Q ExActive mass spectrometer (Thermo Fisher Scientific, Waltham, USA) with the standardized flow of the company.

Primary buffers used in the RAP-MS experiment were listed as follows: Total cell lysis buffer: 10 mmol/L Tris-HCl pH

7.5, 500 mmol/L LiCl, 0.5% dodecyl maltoside, 0.2% sodium dodecyl sulfate, 0.1% sodium deoxycholate, 200 × protease inhibitor cockail (4.6 μL) and 920 U of RNase inhibitor (23 μL). 1.5 × hybridization buffer: 15 mmol/L Tris-HCl pH 7.5, 7.5 mmol/L ethylenediaminetetraacetic acid, 750 mmol/L lithium chloride (LiCl), 0.75% dodecyl-β-d-maltopyranoside (DDM), 0.3% sodium dodecyl sulfate (SDS), 0.15% sodium deoxycholate, 6 mol/L urea, 3.75 mmol/L Tris (2-carboxyethyl) phosphine.

RNA cellular cytoplasm and nuclear distribution

Cell membrane could be disrupted by the lysis buffer (140 mmol/L NaCl, 1.5 mmol/L $MgCl_2$, 10 mmol/L Tris-HCl pH 8.5 and 0.1% Nonidet P-40 [Catalog No. 74385, Sigma]) with an intact nucleus. We harvested about 1×10^6 cells and washed the harvested cells twice with ice-cold PBS. Cells were lysed by 100 μL lysis buffer before icing for 5 min and centrifuged at 800 *g* for 5 min at 4°C. The supernatant was transferred into new tubes for cytoplasm RNA purification. The nucleus pellet needed to wash with PBS for 1–2 times and centrifuge at 800 *g* for 5 min at 4°C. Each 1 mL TRizol was added to the supernatant and pellet samples. RNAs were purified from these samples. The same volume of RNAs (total mass was not >2 μg) was reversed transcription into complementary DNA (cDNA). The ratio of RNA cellular cytoplasm and nuclear distribution could be calculated using real-time polymerase chain reaction (PCR) data.

RIP

RIP was performed following the instructions of the Magna RIP kit (Catalog No. 17-700, Millipore, Darmstadt, Germany). The Vimentin monoclonal antibody (Catalog No. ab8979, Abcam, Cambridge, UK) was used to immunoprecipitate Vimentin–RNAs complexes. Approximately 2 μg of Vimentin antibody and the same amount of homologous immunoglobin (IgG) were used in each RIP experiment.

RNA pull-down assay

Biotin-labeled RNA was transcribed *in vitro* using the MEGAscript T7 Kit (Catalog No. AM1333, Invitrogen) with biotin-uridine triphosphate (Catalog No. R0081, Thermo Scientific) and purified according to the manufacturer's instructions, then incubated with whole-cell lysates. Biotin-labeled transcripts and coprecipitated proteins were isolated with streptavidin beads, subjected to sodium dodecyl sulfate polyacrylamide gel electrophoresis (SDS-PAGE) analysis, and further visualized by immunoblotting assay.

Western blotting

Total protein lysate was isolated using ristocetin-induced platelet aggregation (RIPA) lysis buffer (Catalog No. C1053, Applygen, Beijing, China). For samples eluted from the RIP procedure, 5 × protein loading buffer was added and denatured at 95°C for 5 min. All protein samples were loaded on 10% SDS-PAGE. Proteins were then transferred onto polyvinylidene fluoride (PVDF) membranes (Catalog No. IPVH00010, Millipore). After blocking with 5% non-fat dry milk for 1 h, the membranes were incubated with primary antibody against Vimentin (1:1000, Catalog No. 5741T, CST, Danvers, USA) and glyceraldehyde-3-phosphate dehydrogenase (GAPDH) (1:2000, Catalog No. 60004-1-Ig, Proteintech) at 4°C overnight, respectively. Subsequently, the membranes were incubated with a suitable horseradish peroxidase (HRP)-conjugated secondary antibody for 1 h. After sufficient washing, the blots were detected using an enhanced chemiluminescence imaging system (GE healthcare, Chicago, USA).

Quantitative real-time PCR (qRT-PCR)

RNAs were purified using the ultra RNA purification kit (Kit catalog No. CW0581, CWbiotech, Taizhou, China) and reverse-transcribed into cDNA (Catalog No. RR047Q, TaKaRa, Otsu, Japan) according to the manufacturer's instructions. Real-time PCR was performed using the Applied Bio-systems 7500 Sequence Detection system (Applied Bio-systems, Foster, USA). The CCAT1 (primer: forward, 5′-CATTGGGAAAGGTGCCGAGA-3′; reverse, 5′-ACGCTTAGCCATACAGAGCC-3′), nuclear paraspeckle assembly transcript 1 (NEAT1) (primer: forward, 5′-CCTGCCTTCTTGTGCGTTTC-3′; reverse, 5′-CTTGTACCCTCCCAGCGTTT-3′), and VIM (primer: forward, 5′-CCTCCGGGAGAAATTGCAGG-3′; reverse, 5′-GCGTTCAAGGTCAAGACGTG-3′) were normalized to the mean expression level of GAPDH (primer: forward, 5′-TGCACCACCAACTGCTTAG-3′; reverse, 5′-GACGCAGGGATGATGTTC-3′). $2^{-\Delta\Delta Ct}$ method was used for the analysis of quantitative changes in gene expression.

Cell migration and invasion assay

Cell migration was determined using Transwell cell culture inserts (Catalog No. 3422, CORNING, New York, USA) with a pore size of 8 μm membranes. HeLa cells were transfected with CCAT1 overexpression plasmids or a Smart silencer (RiboBio, Guangzhou, China). Approximately 36 h after transfection, cells (8×10^5/mL) were suspended in 100 μL of serum-free DMEM medium and seeded on the upper compartment of the 24-well Transwell culture chamber. About 650 μL of DMEM medium, including 10% fetal bovine serum, was added to the lower wells. After 12 to 18 h, cells had migrated to the lower side of the membrane, were fixed with methanol, and stained with 2% crystal violet dissolved in methanol. Pictures were taken for cells attached to the membrane, and migrated cells were counted. For the cell invasion assay, 50 μL 2% of Matrigel (Catalog No. 354230, CORNING) dissolved in serum-free DMEM medium was added into the Transwell cell culture inserts evenly. Cell culture inserts were incubated at 37°C for 12 to 18 h.

Bioinformatic analysis

We used the gene expression profiling interactive analysis (GEPIA) website to examine pan-cancer CCAT1 expression.[22] The parameters were set as follows: differential

methods were analysis of variance (ANOVA), Log_2 FC cut-off value is 1, the q-value cut-off value was 0.01, Normal data matching selected match The Cancer Genome Atlas (TCGA) normal and the Genotype-Tissue Expression (GTEx) data. The database for annotation, visualization, and integrated discovery (DAVID) website was used to analyze the gene ontology, pathways, and protein domains features of CCAT1 binding proteins.[23] A total of 631 *Homo sapiens* (*H. sapiens*) CCAT1 binding proteins were screened and arranged accordingly. The official gene symbol was used for webtool analysis. We downloaded *H. sapiens* RBPs from the database for eukaryotic RNA binding proteins (EuRBPDB).[24] We compared CCAT1 binding proteins with the downloaded RBPs to evaluate RAP reliability.

Statistical analysis

All statistical tests were performed using GraphPad Prism (version 7.0 for Windows, www.graphpad.com, GraphPad Software, San Diego, USA). All experiments were independently performed in triplicate, and data were presented as mean ± standard deviation. Statistical analyses were performed using Student's *t*-test and ANOVA. Each *P* value was two-sided, and $P < 0.05$ was considered statistically significant.

Results

CCAT1 overexpressed in multiple cancers and enhanced the migration and invasion abilities of HeLa cells

We used the online TCGA and GTEx projects RNA sequencing analyzing web server GEPIA to analyze CCAT1 expression levels in pan-cancers.[22] The results indicated that CCAT1 was significantly up-regulated in tumor tissues compared with normal tissues across cancers, particularly in rectum adenocarcinoma, colon adenocarcinoma, lung squamous cell carcinoma, and stomach adenocarcinoma [Figure 1A]. As lncRNA's cellular localization is crucial for their roles in cell signaling regulation, CCAT1 expression in cellular cytoplasm and nucleus fractionated RNAs was examined by qRT-PCR, with results indicating CCAT1 distribution in both the cellular cytoplasm and nucleus [Figure 1B]. To explore the biological functions of CCAT1, the overexpression system was constructed to manipulate the CCAT1 expression level [Figure 1C].

Meanwhile, we used the CCAT1 silencer, which is the mixture of small interfering RNA (siRNA) and antisense oligonucleotide (ASO) target for CCAT1, to knock down CCAT1 expression in cells [Figure 1D]. Furthermore, we performed transwell analysis to evaluate the variation of HeLa cells' migration and invasion abilities. Resultantly, a high CCAT1 expression level significantly enhanced HeLa cells' migration and invasion abilities [Figure 1E,F]. Oppositely, CCAT1 knocked down significantly suppressed HeLa cells' migration and invasion abilities [Figure 1G,H]. These results indicated that CCAT1 functioned as an oncogenic lncRNA by contributing to migration and invasion abilities of cancer cells. To further understand the underlying mechanisms that CCAT1 is involved in cancer promotion, we attempted to clarify CCAT1's oncogenic role from the perspective of RNA-protein interaction according to our former understanding of it.

Adapting RAP-MS method to purify and identify CCAT1 binding proteins

RAP-MS is a method that enables the identification of direct and specific protein interaction partners of a specific RNA molecule,[21] which provides proteome-wide high-confidence protein interactors. We adapted two parts of the previously reported method to avoid isotope labeling of amino acids and to enhance the cross-link strength of RNA-protein partners. As depicted in Figure 2A, HeLa and HeLa-Nlp cells were cultured to about 80% confluence. Then 4sU was added into the medium. The cells were treated for 16 h before harvesting. RAP experiment was performed as mentioned in the Section "Methods." The quality control samples were collected during RNA antisense purification (RAP) procedure. RNAs were purified from the quality control samples and converted to complementary DNA (cDNA). Real-time PCR was performed to examine the CCAT1 level in quality control samples. The results showed that probes of the 365 nm wavelength cross-linked groups captured CCAT1 transcripts in finally eluted samples less than 15% of the input samples. However, probes of the 254 nm wavelength cross-linked group captured much more CCAT1 than 365 nm wavelength cross-linked groups. It indicated that the denatured condition might have washed out a large amount of non-specific binding [Figure 2B]. Silver staining for finally eluted protein samples showed that there were much more proteins in 365 nm wavelength UV cross-linked groups than 254 nm wavelength UV cross-linked group [Figure 2C]. These results indicated that the adapted RAP-MS method was effective in purifying CCAT1 binding protein.

Characteristics of CCAT1 binding proteins

The number of CCAT1 binding proteins identified by mass spectrometry in the HeLa cell and HeLa-Nlp cell was 558 and 370 [Supplementary Table 2, http://links.lww.com/CM9/B244], respectively. We then arranged CCAT1 binding proteins using bioinformatics websites DAVID.[23] Gene ontology analyses showed that molecular functions of CCAT1 binding proteins were concentrated not only on protein binding but also on poly(A) RNA binding, adenosine triphosphate binding, and RNA binding [Figure 3A]. Cellular component dimensions showed that these proteins were widely distributed in the primary cell compartment [Figure 3B]. These proteins mainly participated in cell–cell adhesion, oxidation-reduction, and mRNA splicing via spliceosome biological processes [Figure 3C]. Notably, protein domains of CCAT1 binding proteins were primarily clustered in P-loop nucleoside hydrolase, nucleotide-binding, and RRM [Figure 3D]. The KEGG pathways of CCAT1 binding proteins were also evaluated. Most proteins focused on spliceosome, RNA transport, and protein processing in the endoplasmic reticulum [Figure 3E]. Characteristics of CCAT1 binding proteins were in accordance with RBPs. CCAT1 binding proteins were compared with human RBPs recorded by EuRBPDB.[24] In the HeLa group, 21%

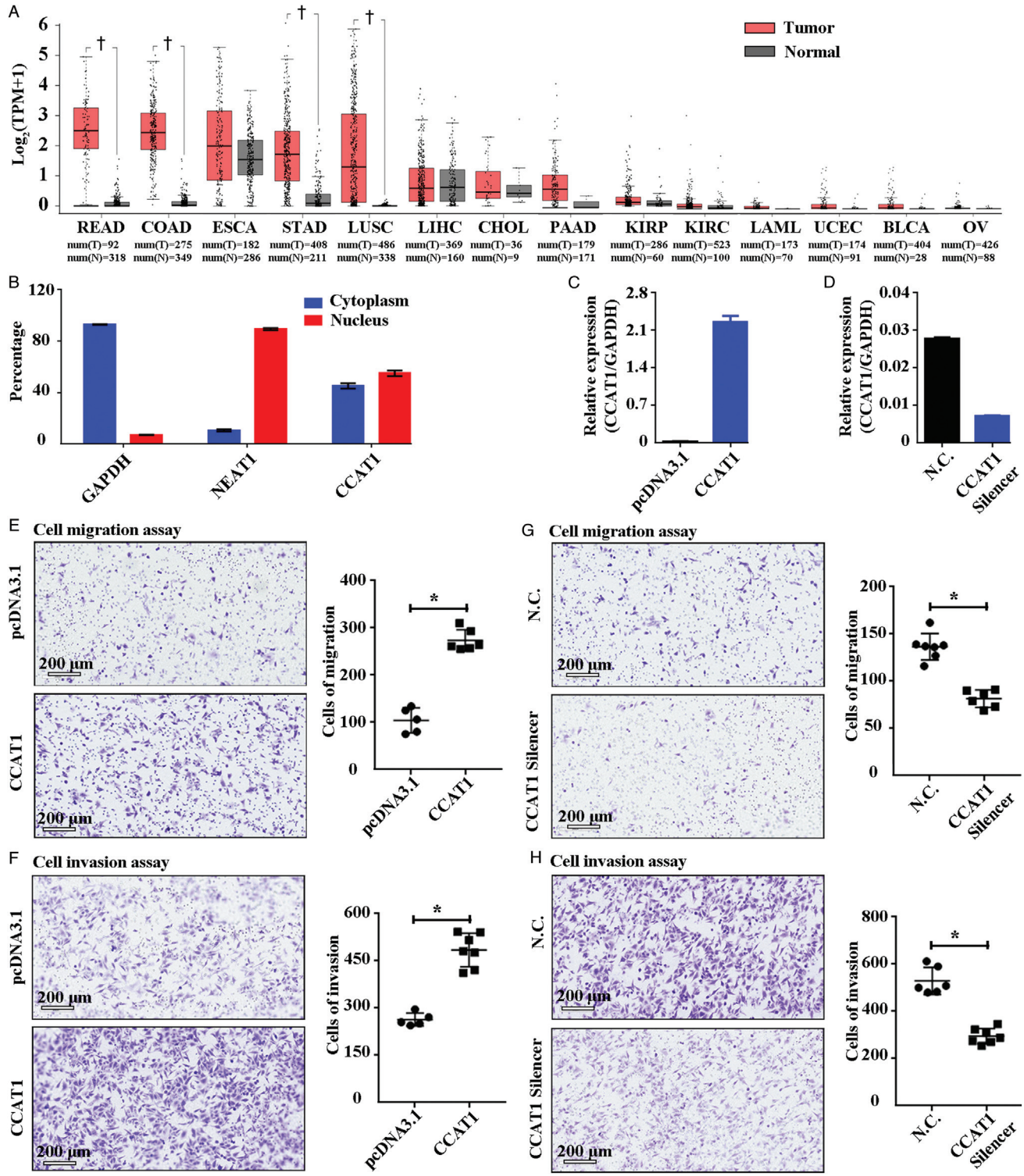

Figure 1: CCAT1 presented a high expression level among multiple cancers and enhanced the migration and invasion abilities of HeLa cells. **(A)** CCAT1 expression pattern analyzed by GEPIA website, CCAT1 was overexpressed in tumor samples compared with normal tissues across human tumors (Cut off *P* value is <0.01, marked as†). **(B)** Cellular cytoplasm and nuclear component of HeLa cells were separated. Total RNA was purified to examine CCAT1 RNA expression level. CCAT1 is localized in both cellular cytoplasm and nucleus. GAPDH and NEAT1 were representatives of cellular cytoplasm and nuclear transcripts, respectively. **(C)** CCAT1 was up-regulated in HeLa cells by transfecting pcDNA3.1-CCAT1 plasmids into cells. **(D)** CCAT1 was knocked down by CCAT1 silencer which contained small interferring RNA and antisense oligonucleotide targeted to CCAT1. GraphPad Prism 7.0. was used to graphically present the RNA quantitative data. N.C. means negative control. **(E,F)** CCAT1 up-regulation significantly enhanced the migration **(E)** and invasion abilities **(F)** of HeLa cells. Hematoxylin and eosin staining **(G,H)** CCAT1 knocked down significantly decreased the migration **(G)** and invasion abilities **(H)** of HeLa cells Hematoxylin and eosin staining. GraphPad Prism 7.0. was used for statistical analysis and graphical present cell number of migration and invasion. * means $P<0.01$ in *t*-test. BLCA: Bladder urothelial carcinoma; CCAT1: Colon cancer-associated transcript 1; CHOL: Cholangio carcinoma; COAD: Colon adenocarcinoma; ESCA: Esophageal carcinoma; GADPH: Glyceraldehyde-3-phosphate dehydrogenase; GEPIA: Gene expression profiling interactive analysis; KIRC: Kidney renal clear cell carcinoma; KIRP: Kidney renal papillary cell carcinoma; LAML: Acute myeloid leukemia; LIHC: Liver hepatocellular carcinoma; LUSC: Lung squamous cell carcinoma; N.C.: Negative control; OV: Ovarian serous cystadenocarcinoma; PAAD: Pancreatic adenocarcinoma; READ: Rectum adenocarcinoma; STAD: Stomach adenocarcinoma; UCEC: Uterine corpus endometrial carcinoma.

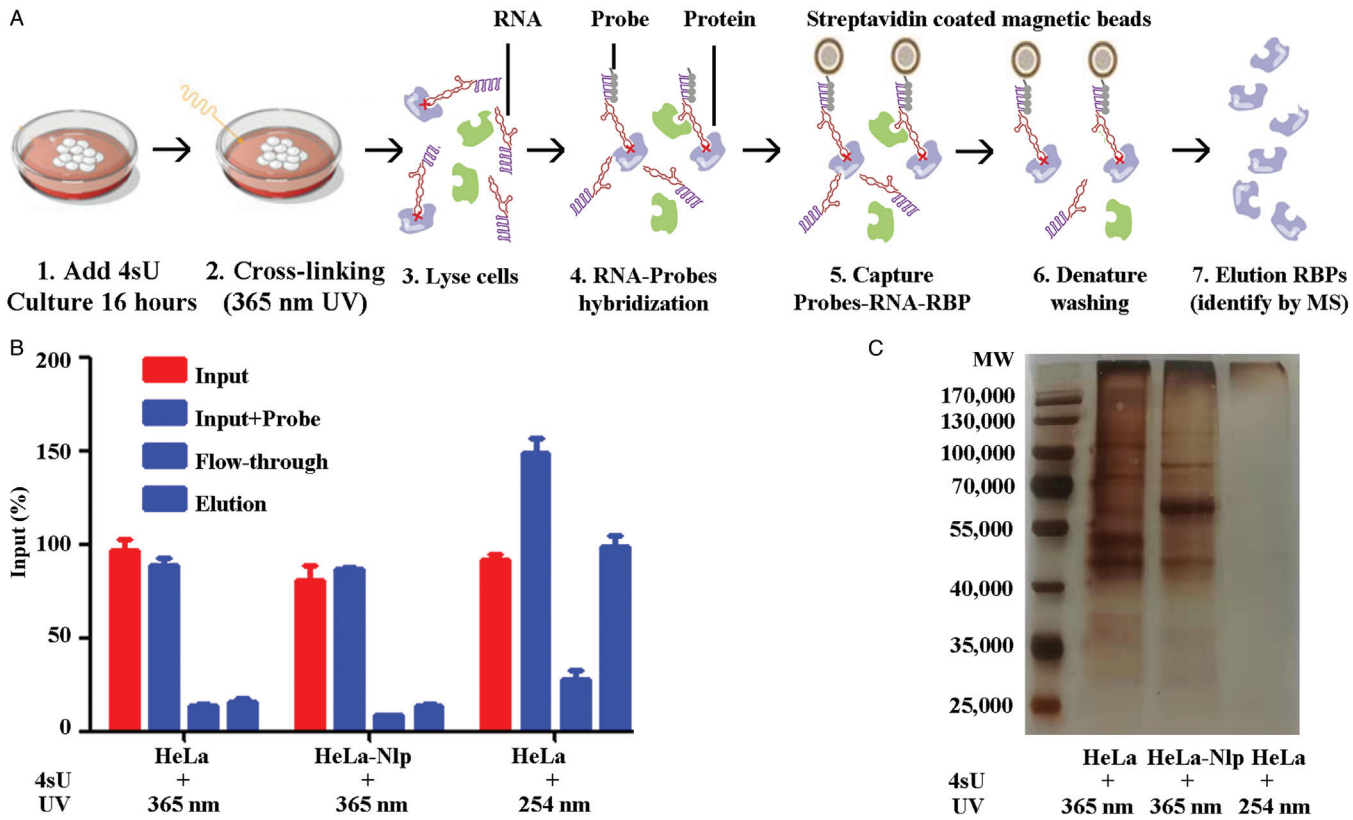

Figure 2: Identifying CCAT1 binding proteins by RAP-MS. **(A)** RAP-MS procedure was adapted from the protocol reported before (RAP-MS Protocol: McHugh *et al*[21]) with two major improvements. First, 4sU was incorporated into transcripts by culturing cells with 4sU containing medium for 16 h. Second, the cross-linking condition was 0.8 J/cm^2 with ultraviolet light 365 nm wavelength. The experimental scheme was depicted above. **(B)** To evaluate CCAT1-probes binding efficiency, CCAT1 level was examined using qRT-PCR. Results showed that probes targeted CCAT1 could bind CCAT1 transcript effectively, and denatured washing procedures were sufficiently in both HeLa and HeLa-Nlp groups (Input, Input + Probe, and Flow-through and Elution). **(C)** Silver staining of RAP purified CCAT1 binding proteins. 4sU: 4-thiouridine; CCAT1: Colon cancer-associated transcript 1; MS: Mass spectrometry; RAP-MS: RNA antisense purification coupled with mass spectrometry; RBPs: RNA binding proteins; qRT-PCR: Quantitative real-time PCR; UV: Ultraviolet.

(116/558) and 39% (220/558) of CCAT1 binding proteins were identified as canonical RBPs and non-canonical RBPs, respectively. In the HeLa-Nlp group, these percentages were 20% (74/370) and 40% (147/370) [Figure 3F]. These proteins were compared with identified CCAT1 binding proteins [Supplementary Table 3, http://links.lww.com/CM9/B245]. Interestingly, Vimentin was the only intersection among the four comparison groups [Figure 3G]. Vimentin is a vital protein that affects the migration and invasion abilities of cancer cells. RIP was performed to validate Vimentin's binding potential to CCAT1. Results showed that the Vimentin antibody could enrich CCAT1 transcripts more precisely than the IgG group [Figure 3H,I]. *In vitro* RNA pull-down test was also performed to pull out Vimentin protein with CCAT1 probe. The result obviously showed that CCAT1 could pulldown Vimentin protein [Figure 3J]. These results validated the CCAT1–Vimentin interaction. However, the influence of their interactions on cancer cells' migration and invasion remained unknown.

Vimentin protein level decreased upon CCAT1 downregulation and the migration and invasion abilities of HeLa cells were weakened

To investigate the influence of CCAT1 on Vimentin expression, CCAT1 was knocked down by a CCAT1 silencer in HeLa cells. We found that reduced CCAT1 expression did not influence Vimentin mRNA levels [Figure 4A]. However, protein level was slightly decreased [Figure 4B]. Former results showed that CCAT1 interfering significantly weakens the migration and invasion abilities of HeLa cells [Figure 1G,H]. We were unsure whether the protein level change of Vimentin could affect the migration and invasion abilities of HeLa cells. Therefore, we down-regulated VIM using siRNA [Figure 4C,D] and observed that HeLa cells' migration and invasion abilities were significantly suppressed [Figure 4E,F]. These effects were equal to CCAT1 downregulation. Further, we needed to validate that CCAT1 functioned by affecting the stability of the Vimentin protein.

CCAT1 enhanced HeLa cells' migration and invasion abilities by affecting Vimentin protein

We had known CCAT1 could affect the protein level of Vimentin from the above results. We needed experiments to validate CCAT1 functions by directly involving Vimentin. We then knocked down *VIM* and rescued the downregulation by overexpressing CCAT1. Consistent with former results, there was no change in the mRNA level of the *VIM* gene upon CCAT1 overexpression [Figure 5A]. But CCAT1 overexpression could weaken the decrease of Vimentin protein upon *VIM* knocked down [Figure 5B]. It indicated that CCAT1 could affect the Vimentin protein. Additionally, CCAT1 overexpression

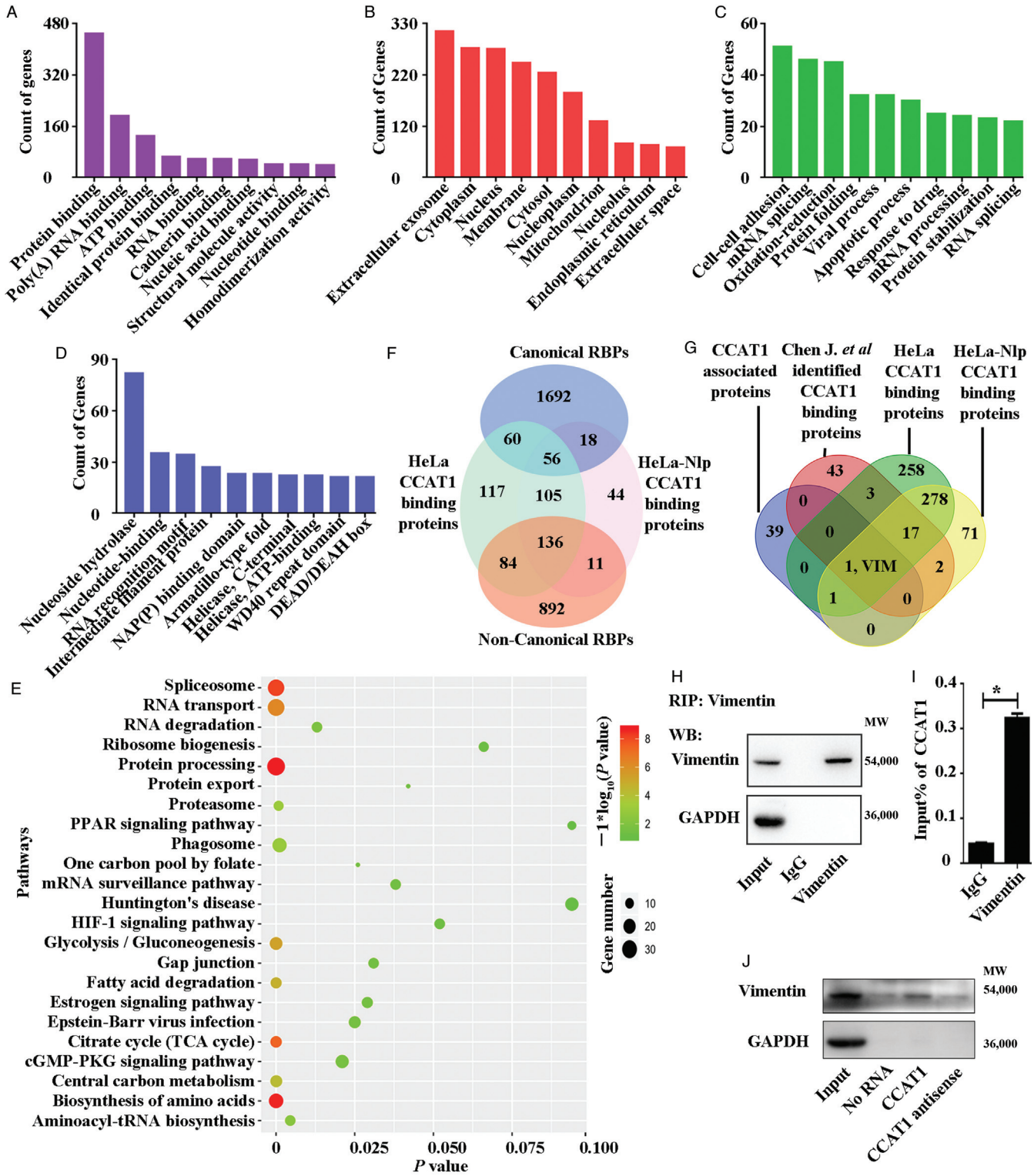

Figure 3: Bioinformatics analysis of CCAT1 binding proteins was identified using RAP-MS. Online bioinformatics web tool DAVID was used for analyzing biological meaning of CCAT1 binding proteins. Gene ontology analysis was presented: **(A)** molecular function, **(B)** cellular component, and **(C)** biological process. **(D)** The top 10 enriched protein domains of CCAT1 binding proteins were arranged and shown. **(E)** KEGG pathways CCAT1 participated mainly focused on spliceosome, protein processing, and RNA transport. **(F)** Comparison of CCAT1 binding proteins with human RBPs (recorded by EuRBPDB database) was shown. **(G)** Comparison of CCAT1 binding proteins, CCAT1-related proteins, and Chen *et al*[25] identified CCAT1 binding proteins. Vimentin is the only common protein. **(H,I)** Vimentin RIP was performed to validate the binding of Vimentin–CCAT1. Vimentin protein could be detected in Vimentin RIP complexes **(H)**. RNAs were purified from Vimentin RIP complexes and inverse transcripted into cDNA. **(I)** The real-time PCR result showed that CCAT1 was significantly enriched by Vimentin. **(J)***In vitro* RNA pull-down test was performed to validate CCAT1–Vimentin protein interaction with CCAT1 probe. GraphPad Prism 7.0. was used for statistical analysis and graphical present CCAT1 enrichment percentage in RIP. * means $P<0.01$ in *t*-test. CCAT1: Colon cancer-associated transcript 1; DAVID: Database for annotation, visualization, and integrated discovery; EuRBPDB: Database for eukaryotic RAP-MS: RNA antisense purification coupled with mass spectrometry; RNA binding proteins; RBPs: RNA binding proteins; RIP: RNA immunoprecipitation; mRNA: massage ribonucleic acid; ATP: Adenosine triphosphate; DEAD/DEAH box: (DEAD, Asp-glu-ala-glu or DEAH, asp-glu-ala-his) protein domains; HIF-1: Hypoxia-inducible factor-1; GAPDH: Glyceraldehyde-3-Phosphate Dehydrogenase; TCA cycle: Tricarboxylic acid cycle; KEGG: Kyoto Encyclopedia of Genes and Genomes; PCR: Polymerase chain reaction. [25] Chen J, Alduais Y, Zhang K, Zhu X, Chen B. CCAT1/FABP5 promotes tumour progression through mediating fatty acid metabolism and stabilizing PI3K/AKT/mTOR signalling in lung adenocarcinoma. J Cell Mol Med 2021;25:9199–9213. doi: 10.1111/jcmm.16815.

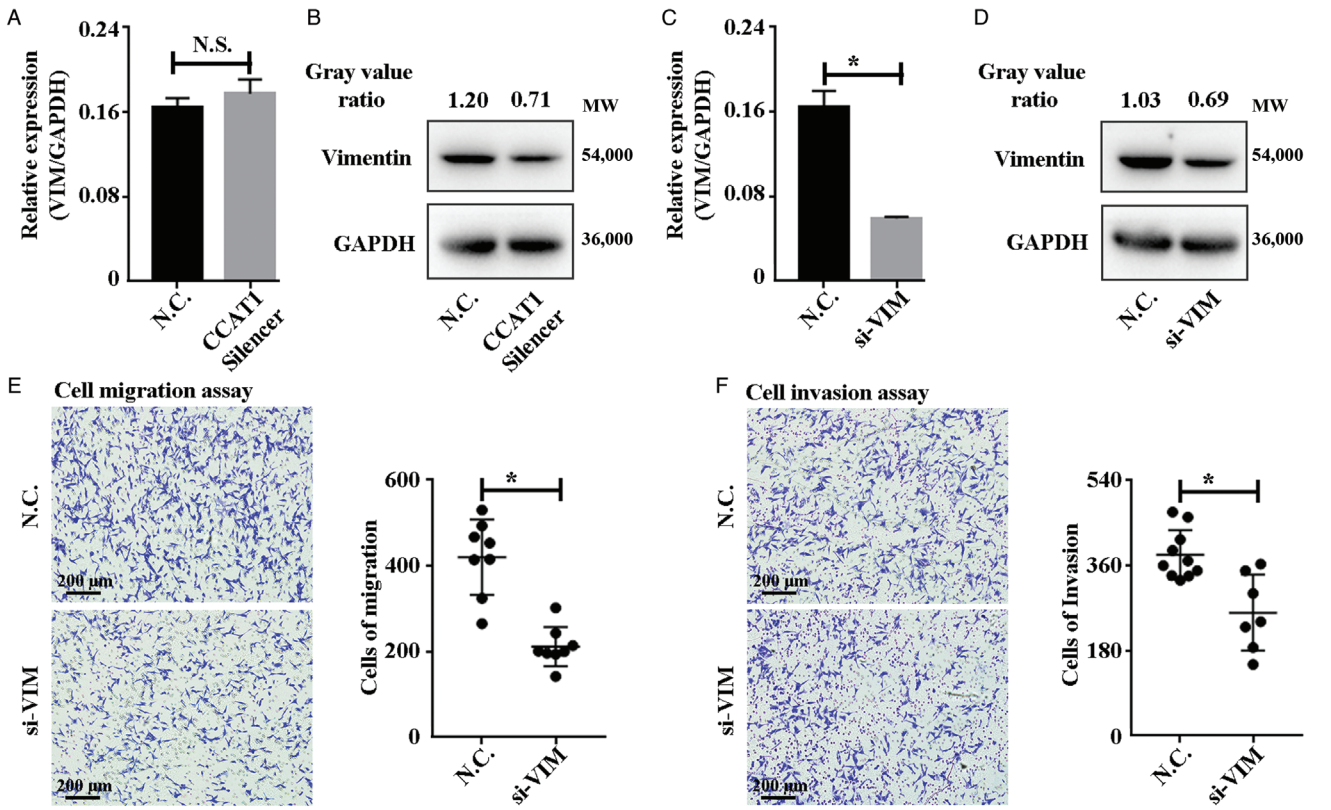

Figure 4: VIM-depleted weakened HeLa cells' migration and invasion abilities. **(A)** CCAT1 downregulation did not influence the mRNA expression level of *VIM* gene. **(B)** Vimentin protein level was decreased accompanied by CCAT1 down-regulation. **(C)** *VIM* gene was downregulated using RNA interfering technique. The mRNA expression level of *VIM* gene was downregulated successfully. **(D)** Vimentin protein level was downregulated successfully using RNA interfering technique (right). **(E)** VIM knocked down significantly weakened HeLa cells' migration ability. **(F)** VIM knocked down significantly weakened HeLa cells' invasion ability. GraphPad Prism 7.0. was used for statistical analysis and graphical present cell number of migration and invasion. * means $P<0.01$ in *t*-test. CCAT1: Colon cancer-associated transcript 1. N.C. means negative control. N.S. means no significance; si-VIM mRNA: small interference RNA targeted VIM massage ribonucleic acid.

could significantly recover the migration and invasion abilities of HeLa cells weakened by knocking down the *VIM* gene [Figure 5C–F]. These results, to some extent, suggested that CCAT1 is bound to Vimentin and enhanced Vimentin protein stability. Resultantly, CCAT1-Vimentin interaction enhanced the migration and invasion abilities of HeLa cells.

Discussion

Elevated CCAT1 expression is involved in tumorigenesis and the development of multiple human cancers.[1] CCAT1 overexpression also showed a positive correlation with primary solid tumors' clinical features and prognosis.[2] CCAT1 plays a critical role in various biological processes, including proliferation, invasion, migration, drug resistance, and survival.[1,3,4,8] Mechanistically, CCAT1 could combine with TP63 and SOX2 to co-localize the super-enhancer of epidermal growth factor receptor (EGFR). In this way, the CCAT1–TP63–SOX2 complex could activate EGFR transcription and promote squamous cell carcinoma progression.[7] Another study proposed that CCAT1 serves as a scaffold for two distinct epigenetic modification complexes, PRC2 and SUV39H1, and modulates the histone methylation of *SPRY4* promoter in the nucleus.[26] Thus, CCAT1 promotes cell growth and migration. These discoveries provided proof of CCAT1's protein binding ability. However, further study is required to clarify the mechanism of CCAT1's biological functions, particularly from the CCAT1-protein interaction dimension.

Notably, RAP-MS could purify and identify proteome-wide RNA-binding partners. Ultraviolet light was used to cross-link for RNA and protein partners. Additionally, stable isotope labeling of amino acids in cell culture tagging could be a useful approach to compare multiple protein capturing samples using a single mass spectrometry experiment.[13,21]. However, this approach has been limited in most laboratories due to forbidden isotope labeling. Thus, the incorporation of highly photoreactive nucleosides 4sU into newly transcribed RNAs in living cells could solve this problem. Upon irradiating with 365 nm wavelength UV light, cross-linking of 4sU-labeled RNAs to aromatic amino acid side chains of the interacting RBPs was achieved.[27] Adapted RAP-MS methods were used to successfully purify CCAT1 binding proteins in our experiment. Even though the CCAT1 transcript bound to probes in the last elution sample was <15% of the mass of the input. But the silver staining results indicated that enough proteins were purified. These proteins could be identified by mass spectrometry. These data showed that 4sU incorporation and 365 nm UV cross-linking enabled RNA-protein interaction complexes to endure more stringent washing conditions and identify specific binding partners.

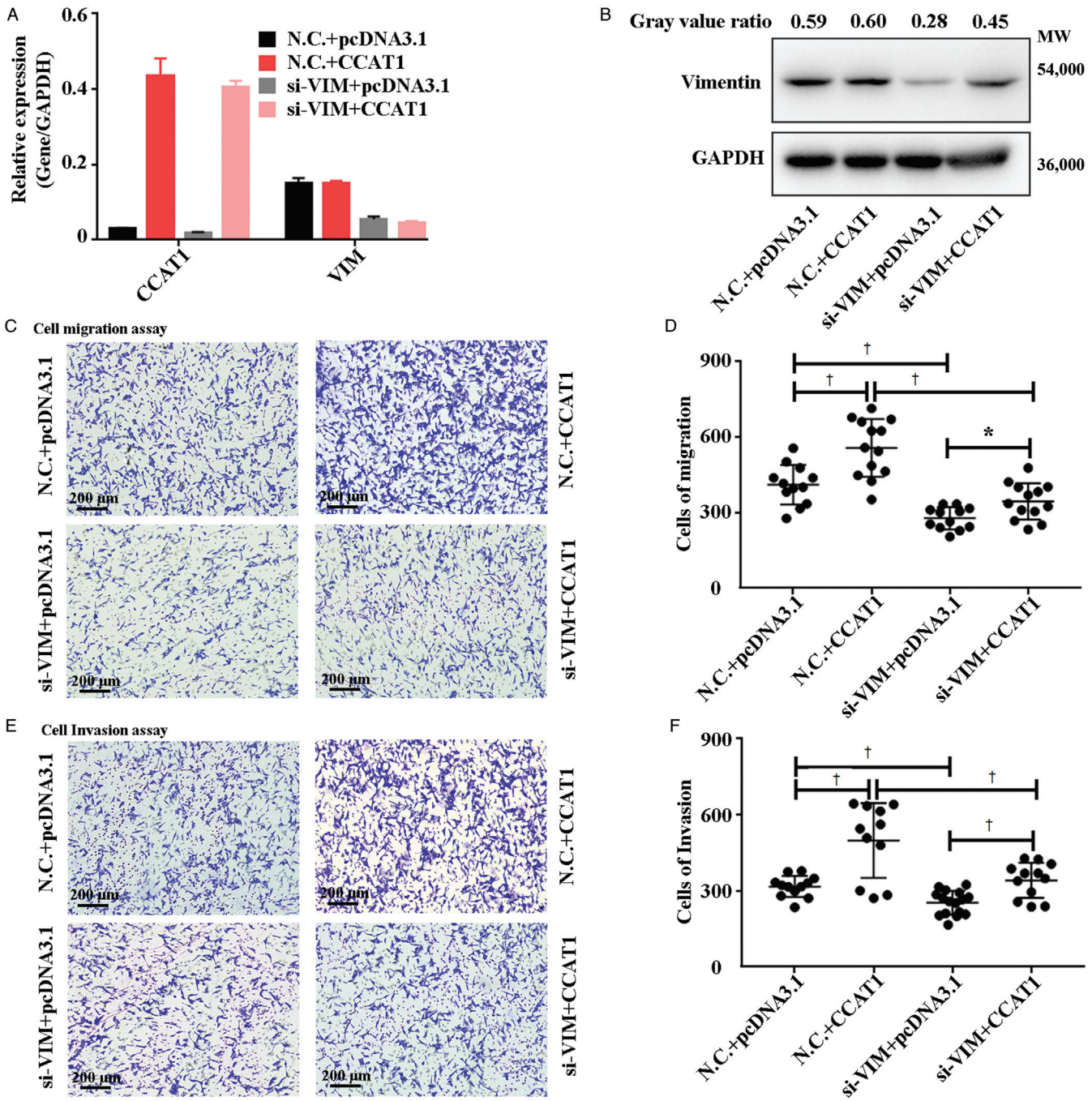

Figure 5: CCAT1 affected Vimentin protein level and enhanced cancer cells' migration and invasion abilities. Recovery assay was performed to validate the binding between CCAT1 and Vimentin protein. CCAT1 up-expression plasmids and siRNA targeted to VIM mRNA were co-transfected into HeLa cells. **(A)** CCAT1 expression level increased obviously in CCAT1 plasmids transfected groups. CCAT1 over-expression did not affect the VIM mRNA level. VIM mRNA level decreased obviously in VIM-depleted groups without affecting CCAT1 expression level. **(B)** Western blotting examined the protein level of Vimentin. **(C–F)** Cell migration assays were performed for the above co-transfected HeLa cells. **(D)** Cell number was counted and statistically analyzed using GraphPad Prism software V7.0. VIM knocked down significantly weakened the migration ability of HeLa cells. This appearance could be reverted by increasing CCAT1 expression level by transfecting CCAT1 plasmids. **(E)** Cell invasion assays were performed for the above co-transfected HeLa cells. Cell numbers were counted and statistically analyzed using GraphPad Prism software V7.0. **(F)** VIM knocked down significantly weakened the invasion ability of HeLa cells. This appearance could be reverted by increasing CCAT1 expression level by transfecting CCAT1 plasmids. *means $P < 0.05$ and †means $P < 0.01$ in analysis of variance. CCAT1: Colon cancer-associated transcript 1. N.C. means negative control; mRNA: massage ribonucleic acid; GAPDH: Glyceraldehyde-3-Phosphate Dehydrogenase.

CCAT1 binding proteins, including CTCF,[28] TP63, SOX2,[7] and PRC2[26] reported by previous studies, were not presented in our RAP-MS identified protein list. It is worth mentioning that these studies adopted RIP and *in vitro* RNA pull-down methods to identify RNA-protein interactions. These two *in vitro* methods simulated the physiological environment of cells to perform RIP and RNA pull-down. Therefore, these conditions might help molecules with a greater probability of binding partners isolated by cellular spatial structure.[26] In this study, >60% of CCAT1 binding proteins identified by RAP-MS were RBPs recorded by EuRBPDB online database. However, further studies to verify our method in specific cell physiological conditions and more cancer types are needed.

Vimentin is a significant constituent of the intermediate filament family of proteins. It is known to maintain cellular integrity and provide resistance against stress. Elevated Vimentin protein expression has been reported in various epithelial cancers, including prostate cancer, gastrointestinal tumors, central nervous system tumors, breast cancer, and other cancer types.[29,30] Most studies have found that Vimentin mainly functions in the EMT, cell migration, and invasion.[16] Previously, lncRNA-Dreh, lncRNA-AOC4P, and LINC00675 were demonstrated to combine with Vimentin and repress its expression, inhibiting tumor metastasis.[18,19,31] In contrast, lncRNA BC088259 promoted Schwann cell migration through Vimentin following peripheral nerve injury.[17] Recently, Vimentin was also recorded by EuRBPDB and classified into non-canonical RBPs. In our study, Vimentin was identified as a CCAT1 binding protein. CCAT1 binds with Vimentin and enhances its stability. Resultantly, the CCAT1–Vimentin interaction promoted HeLa cell migration and invasion.

In this study, we concentrated on methodological developing of RAP-MS for RBPs identification. We successfully established the approach and efficiently validated CCAT1-Vimentin interactions in HeLa cells. We demonstrated that CCAT1 binds with Vimentin and affected its protein expression level. Meanwhile, we also realized the limitation of our study that the investigation was only carried out in HeLa cell line. The validations of the RAP-MS in pan-cancer cells have not started yet. According to the excellent performance of methodology we established, we believe that the RAP-MS can also be used in other different cancer cells and we will prove this in pan-cancer cells in the future study.

In conclusion, a RAP-MS approach was adapted to purify and identify proteome-wide lncRNA directly binding proteins. This method might help to understand the key molecular regulation mechanism of biology on the RNA-protein interaction. CCAT1 could bind and affect Vimentin protein resulted in enhancing the migration and invasion abilities of cancer cells. These findings may help target RNAs and proteins at the same time in future oncotherapy.

Funding

This work was supported by grants from the Sanming Project of Medicine in Shenzhen (No. SZSM201612021), Special Foundation for Science and Technology Development of Guangdong Province (No. 2017B090904010), Scientific Research Project of Health and Family Planning Commission of Shenzhen Municipality (No. SZXJ2018086), and the Science and Technology Development Fund Project of Shenzhen (Nos. JCYJ20190809100217290 and JCYJ20190809095801653).

Conflicts of interest

None.

Data availability

Mass spectrometry proteomics data have been deposited to the ProteomeXchange Consortium (http://www.proteomexchange.org/) via the iProX partner repository with the dataset identifier PXD022774.

References

1. Xin Y, Li Z, Shen J, Chan MTV, Wu WK. CCAT1: a pivotal oncogenic long non-coding RNA in human cancers. Cell Prolif 2016;49:255–260. doi: 10.1111/cpr.12252.
2. Zhang Z, Xie H, Liang D, Huang L, Liang F, Qi Q, *et al*. Long non-coding RNA CCAT1 as a diagnostic and prognostic molecular marker in various cancers: a meta-analysis. Oncotarget 2018;9:23695–23703. doi: 10.18632/oncotarget.24923.
3. Shan L, Liu W, Zhan Y. Long non-coding RNA CCAT1 acts as an oncogene and promotes sunitinib resistance in renal cell carcinoma. Front Oncol 2020;10:516552. doi: 10.3389/fonc.2020.516552.
4. Gu C, Zou S, He C, Zhou J, Qu R, Wang Q, *et al*. Long non-coding RNA CCAT1 promotes colorectal cancer cell migration, invasiveness and viability by upregulating VEGF via negative modulation of microRNA-218. Exp Ther Med 2020;19:2543–2550. doi: 10.3892/etm.2020.8518.
5. Liu Z, Chen Q, Hann SS. The functions and oncogenic roles of CCAT1 in human cancer. Biomed Pharmacother 2019;115:108943. doi: 10.1016/j.biopha.2019.108943.
6. Cui R, Liu C, Lin P, Xie H, Wang W, Zhao J, *et al*. LncRNA AC245100. 4 binds HSP90 to promote the proliferation of prostate cancer. Epigenomics 2020;12:1257–1271. doi: 10.2217/epi-2020-0270.
7. Jiang Y, Jiang YY, Xie JJ, Mayakonda A, Hazawa M, Chen L, *et al*. Co-activation of super-enhancer-driven CCAT1 by TP63 and SOX2 promotes squamous cancer progression. Nat Commun 2018;9:3619. doi: 10.1038/s41467-018-06081-9.
8. Han C, Li X, Fan Q, Liu G, Yin J. CCAT1 promotes triple-negative breast cancer progression by suppressing miR-218/ZFX signaling. Aging (Albany NY) 2019;11:4858–4875. doi: 10.18632/aging.102080.
9. Zhang S, Xiao J, Chai Y, Du YY, Liu Z, Huang K, *et al*. LncRNA-CCAT1 promotes migration, invasion, and EMT in intrahepatic cholangiocarcinoma through suppressing miR-152. Dig Dis Sci 2017;62:3050–3058. doi: 10.1007/s10620-017-4759-8.
10. Corley M, Burns MC, Yeo GW. How RNA-binding proteins interact with RNA: molecules and mechanisms. Mol Cell 2020;78:9–29. doi: 10.1016/j.molcel.2020.03.011.
11. Hentze MW, Castello A, Schwarzl T, Preiss T. A brave new world of RNA-binding proteins. Nat Rev Mol Cell Biol 2018;19:327–341. doi: 10.1038/nrm.2017.130.
12. Albihlal WS, Gerber AP. Unconventional RNA-binding proteins: an uncharted zone in RNA biology. FEBS Lett 2018;592:2917–2931. doi: 10.1002/1873-3468.13161.
13. McHugh CA, Guttman M. RAP-MS: a method to identify proteins that interact directly with a specific RNA molecule in cells. Methods Mol Biol 2018;1649:473–488. doi: 10.1007/978-1-4939-7213-5_31.
14. Munschauer M, Nguyen CT, Sirokman K, Hartigan CR, Hogstrom L, Engreitz JM, *et al*. The NORAD lncRNA assembles a topoisomerase complex critical for genome stability. Nature 2018;561:132–136. doi: 10.1038/s41586-018-0453-z.
15. Strouhalova K, Prechová M, Gandalovičová A, Brábek J, Gregor M, Rosel D. Vimentin intermediate filaments as potential target for cancer treatment. Cancers 2020;12:184. doi: 10.3390/cancers12010184.
16. Ivaska J, Pallari HM, Nevo J, Eriksson JE. Novel functions of vimentin in cell adhesion, migration, and signaling. Exp Cell Res 2007;313:2050–2062. doi: 10.1016/j.yexcr.2007.03.040.
17. Yao C, Chen Y, Wang J, Qian T, Feng W, Chen Y, *et al*. LncRNA BC088259 promotes Schwann cell migration through vimentin following peripheral nerve injury. Glia 2020;68:670–679. doi: 10.1002/glia.23749.
18. Zeng S, Xie X, Xiao YF, Tang B, Hu CJ, Wang SM, *et al*. Long non-coding RNA LINC00675 enhances phosphorylation of vimentin on Ser83 to suppress gastric cancer progression. Cancer Lett 2018;412:179–187. doi: 10.1016/j.canlet.2017.10.026.
19. Huang JF, Guo YJ, Zhao CX, Yuan SX, Wang Y, Tang GN, *et al*. Hepatitis B virus X protein (HBx)-related long non-coding RNA (lncRNA) down-regulated expression by HBx (Dreh) inhibits hepatocellular carcinoma metastasis by targeting the intermediate filament protein vimentin. Hepatology 2013;57:1882–1892. doi: 10.1002/hep.26195.

20. Zhao X, Jin S, Song Y, Zhan Q. Cdc2/cyclin B1 regulates centrosomal Nlp proteolysis and subcellular localization. Cancer Biol Ther 2010;10:945–952. doi: 10.4161/cbt.10.9.13368.
21. McHugh CA, Chen CK, Chow A, Surka CF, Tran C, McDonel P, *et al*. The Xist lncRNA interacts directly with SHARP to silence transcription through HDAC3. Nature 2015;521:232–236. doi: 10.1038/nature14443.
22. Tang Z, Li C, Kang B, Gao G, Li C, Zhang Z. GEPIA: a web server for cancer and normal gene expression profiling and interactive analyses. Nucleic Acids Res 2017;45:W98–W102. doi: 10.1093/nar/gkx247.
23. Dennis GJ, Sherman BT, Hosack DA, Yang J, Gao W, Lane HC, *et al*. DAVID: database for annotation, visualization, and integrated discovery. Genome Biol 2003;4:3. doi: 10.1186/gb-2003-4-9-r60.
24. Liao JY, Yang B, Zhang YC, Wang XJ, Ye Y, Peng JW, *et al*. EuRBPDB: a comprehensive resource for annotation, functional and oncological investigation of eukaryotic RNA binding proteins (RBPs). Nucleic Acids Res 2020;48:D307–D313. doi: 10.1093/nar/gkz823.
25. Chen J, Alduais Y, Zhang K, Zhu X, Chen B. CCAT1/FABP5 promotes tumour progression through mediating fatty acid metabolism and stabilizing PI3K/AKT/mTOR signalling in lung adenocarcinoma. J Cell Mol Med 2021;25:9199–9213. doi: 10.1111/jcmm.16815.
26. Zhang E, Han L, Yin D, He X, Hong L, Si X, *et al*. H3K27 acetylation activated-long non-coding RNA CCAT1 affects cell proliferation and migration by regulating SPRY4 and HOXB13 expression in esophageal squamous cell carcinoma. Nucleic Acids Res 2017;45:3086–3101. doi: 10.1093/nar/gkw1247.
27. Garzia A, Meyer C, Morozov P, Sajek M, Tuschl T. Optimization of PAR-CLIP for transcriptome-wide identification of binding sites of RNA-binding proteins. Methods 2017;118-119:24–40. doi: 10.1016/j.ymeth.2016.10.007.
28. Xiang JF, Yin QF, Chen T, Zhang Y, Zhang XO, Wu Z, *et al*. Human colorectal cancer-specific CCAT1-L lncRNA regulates long-range chromatin interactions at the MYC locus. Cell Res 2014;24:513–531. doi: 10.1038/cr.2014.35.
29. Sharma P, Alsharif S, Fallatah A, Chung BM. Intermediate filaments as effectors of cancer development and metastasis: a focus on keratins, vimentin, and nestin. Cells 2019;8:497. doi: 10.3390/cells8050497.
30. Satelli A, Li S. Vimentin as a potential molecular target in cancer therapy or vimentin, an overview and its potential as a molecular target for cancer therapy. Cell Mol Life Sci 2011;68:3033–3046. doi: 10.1007/s00018-011-0735-1.
31. Wang TH, Lin YS, Chen Y, Yeh CT, Huang YL, Hsieh TH, *et al*. Long non-coding RNA AOC4P suppresses hepatocellular carcinoma metastasis by enhancing vimentin degradation and inhibiting epithelial-mesenchymal transition. Oncotarget 2015;6:23342–23357. doi: 10.18632/oncotarget.4344.

How to cite this article: Li Z, Yuan J, Da Q, Yan Z, Qu J, Li D, Liu X, Zhan Q, Liu J. Long non-coding RNA colon cancer-associated transcript 1-Vimentin axis promoting the migration and invasion of HeLa cells. Chin Med J 2023;136:2351–2361. doi: 10.1097/CM9.0000000000002373